

Structure Determination and Refinement of Acid Strontium Oxalate from X-Ray and Neutron Powder Diffraction

G. Vanhoyland,^{*,1} F. Bourée,[†] M. K. Van Bael,^{*} J. Mullens,^{*} and L. C. Van Poucke^{*}

^{*}Laboratory of Inorganic and Physical Chemistry, IMO, Limburgs Universitair Centrum, 3590 Diepenbeek, Belgium; and [†]Laboratoire Léon Brillouin (CEA-CNRS), CEA/Saclay, 91191 Gif-sur-Yvette, France

Received August 8, 2000; in revised form November 14, 2000; accepted December 8, 2000

The structure of acid strontium oxalate $\text{Sr}(\text{HC}_2\text{O}_4) \cdot \frac{1}{2}(\text{C}_2\text{O}_4) \cdot \text{H}_2\text{O}$ has been determined by conventional X-ray powder diffractometry. The diffraction pattern was indexed from a monoclinic unit cell with cell parameters $a = 6.341(1) \text{ \AA}$, $b = 16.880(2) \text{ \AA}$, $c = 5.7798(8) \text{ \AA}$, and $\beta = 97.60(1)^\circ$; space group, $P2_1/n$ (No. 14) with $Z = 4$. Final (isotropic) Rietveld refinement of the neutron powder data yielded $R_B = 4.57\%$, $R_F = 2.87\%$, and $R_{wp} = 7.87\%$ as conventional Rietveld parameters. Strontium is eight-fold coordinated and can be described as a distorted bicapped trigonal prism. The SrO_8 polyhedra form one-dimensional chains along the c -axis by sharing edges. In contrast to all other known strontium oxalates, in this compound H_2O acts as bridging ligand between two Sr atoms. SDPD-D classification (1): $\text{Sr}(\text{HC}_2\text{O}_4) \cdot \frac{1}{2}(\text{C}_2\text{O}_4) \cdot \text{H}_2\text{O}$, $P2_1/n$, $C1 = 14$, $Nc = 42$, $C2 = 11$, $\text{XC1} + \text{N/TREOR-97}$ & DICVOL-91 , EXTRA , EQUI , SIRPOW-92 (DM), GFOURIER , FULLPROF . © 2001 Academic Press

Key Words: X-ray powder diffraction; neutron powder diffraction; oxalate; structure determination; Rietveld refinement.

INTRODUCTION

By varying the experimental conditions, different strontium oxalate salts can be obtained. The crystallographic structures of anhydrous SrC_2O_4 (2), $\text{SrC}_2\text{O}_4 \cdot \text{H}_2\text{O}$, and $\text{SrC}_2\text{O}_4 \cdot 2\text{H}_2\text{O}$ (3) have been determined before. From thermal analysis experiments (4) it was clear, however, that by increasing the $[\text{H}_2\text{C}_2\text{O}_4]/[\text{Sr}^{2+}]$ ratio, another pure oxalate can be precipitated with suggested formula $\text{SrC}_2\text{O}_4 \cdot \frac{1}{2}\text{H}_2\text{C}_2\text{O}_4 \cdot \text{H}_2\text{O}$. This compound occurred frequently in oxalate precursors for the $\text{Bi}_2\text{Sr}_2\text{CaCu}_2\text{O}_{8+\delta}$ superconductor and the $\text{La}_{1-x}\text{Sr}_x\text{CoO}_3$ ionic electrolyte. In these multimetal systems, it precipitates separately and in this way decreases the homogeneity of the precursors. In order to find a way to circumvent this problem, a study was

undertaken to determine the structure of the material by powder diffraction.

EXPERIMENTAL

The synthesis was performed in a thermostated cage (25°C) under continuous stirring. The compound was obtained by a double jet mixing of two solutions containing respectively 0.2 M $\text{Sr}(\text{NO}_3)_2$ (Merck) and 1.0 M $\text{H}_2\text{C}_2\text{O}_4 \cdot 2\text{H}_2\text{O}$ (Merck). After complete junction, the solution was allowed to stay for half an hour before being filtered with a 0.2- μm Millipore filter. The white powder was then dried in air. The density of the powder was obtained by pycnometry. Before being used in X-ray diffraction experiments, the powder was lightly ground in a mortar and sieved to pass a 45- μm (325 mesh) sieve. The deuterated compound was synthesized in the same way, but in a glove box under a nitrogen atmosphere, using 0.2 M $\text{Sr}(\text{NO}_3)_2$ (Merck) and 1.0 M $\text{D}_2\text{C}_2\text{O}_4 \cdot 2\text{D}_2\text{O}$ (Aldrich, 99%) in D_2O (Cambridge Isotope Laboratories Inc., 99.9%). The reason for using the deuterated oxalate in the neutron diffraction experiment is that H makes a rather high contribution to the background level since it is a strong incoherent scatterer in neutron diffraction. The quality of the synthesized powders was checked by Thermogravimetric analysis and compared with the results in Ref. (4).

All X-ray experiments (XPD) were performed on a Siemens D-5000 diffractometer (30 mA/40 kV; Bragg–Brentano reflection geometry with 1-mm divergence slit, 2-mm antiscatter slit, and 0.2-mm detector slit) equipped with a Ge(111) incident beam monochromator and a scintillation detector. In the first experiment, the sample was top-loaded and pressed with a glass slit in order to obtain a smooth surface. The powder diffraction pattern was recorded from 8° to $70^\circ 2\theta$, with a step size of $0.01^\circ 2\theta$ and 20 s/step. Peak positions were extracted by peak fitting in the program PROFILE (Siemens). Those peak positions were corrected by applying a correction curve obtained from

¹To whom correspondence should be addressed. Fax: +32-11-26.83.01. E-mail: geert.vanhoyland@luc.ac.be.

TABLE 1
Crystallographic Data for $\text{Sr}(\text{HC}_2\text{O}_4) \cdot \frac{1}{2}(\text{C}_2\text{O}_4) \cdot \text{H}_2\text{O}$

Formula weight ($\text{g}\cdot\text{mol}^{-1}$)	238.6725
Crystal system	Monoclinic
a (Å)	6.341(1)
b (Å)	16.880(2)
c (Å)	5.7798(8)
β (°)	97.60(1)
V (Å ³)	613.2(8)
M_{20}	52
F_{30}	78 (0.0081, 48)
ρ_{obs} ($\text{g}\cdot\text{cm}^{-3}$)	2.5501(9)
Z	3.95 (~ 4)
Space group	$P2_1/n$ (No. 14)

a previously measured external standard SRM 675 (NIST). Crystallographic data are summarized in Table 1.

In the second experiment, the sample was loaded in a side-drifted way in order to minimize possible preferred orientation effects. The diffraction pattern was recorded from 8° to 120° 2θ with a step size of 0.02° 2θ and 30 s/step. This diffraction pattern was used for direct methods and Rietveld refinement.

The neutron powder diffraction experiment (NPD) was done at the Laboratoire Léon Brillouin (LLB) on diffractometer 3T2. The sample (about 3.4 g) was loaded in a vanadium container of 9 mm diameter and 50 mm height. Bragg contributions were measured for 24 hours from 6° to 125.7° 2θ with a step size of 0.05° using a wavelength of

TABLE 2
Details of the Rietveld Refinement

	XPD	NPD
Wavelength (Å)	1.54056	1.2251
2θ range (°)	8–120	6–125.7
Step size (°)	0.02	0.05
No. of reflections	909	1964
No. of profile parameters	18	16
No. of structural parameters	36	56
No. of atoms	11	14
Background	Polynomial (6 coefficients)	Polynomial (4 coefficients)
Cagliotti parameters	$U = 0.188(8)$ $V = -0.040(4)$ $W = 0.0160(6)$	$U = 0.41(1)$ $V = -0.53(1)$ $W = 0.244(4)$
R_F (%) ^a	3.79	2.87
R_B (%) ^a	5.48	4.57
R_{wp} (%) ^a	16.5	7.87

^a All (conventional) R -factors are defined using background-corrected data.

TABLE 3
Atomic Coordinates and Thermal Parameters with Their Standard Deviations for the X-Ray Model

Atom	x	y	z	B_{iso} (Å ²)
Sr	0.8793(2)	0.41798(8)	0.7356(3)	1.25(4)
C1	0.632(2)	0.2392(8)	0.578(3)	1.4(2)
C2	0.583(2)	0.5164(9)	0.093(2)	1.4(2)
C3	0.648(2)	0.2778(8)	0.347(3)	1.4(2)
O1	0.622(1)	0.2287(5)	0.157(2)	1.61(9)
O2	0.673(1)	0.2813(5)	0.756(2)	1.61(9)
Ow3 ^a	0.856(1)	0.5661(5)	0.576(1)	1.61(9)
O4	0.779(1)	0.5085(5)	0.070(1)	1.61(9)
O5	0.575(1)	0.1676(5)	0.569(2)	1.61(9)
O6	0.524(1)	0.5548(4)	0.265(1)	1.61(9)
O7	0.694(1)	0.3488(5)	0.329(1)	1.61(9)

^a Index w is used to indicate the atoms composing the water molecule.

1.2251 Å. These data were used for assigning deuterium positions and Rietveld refinement. Calculation of bond lengths and angles was performed using the NPD model.

RESULTS

X-Ray Powder Diffraction (XPD)

The corrected peak positions were fed into TREOR97 (5) and DICVOL91 (6). Both yielded the same monoclinic result with $M(20) = 52$ and $F(30) = 78$ (0.0081, 48). The unit cell parameters were subsequently least-squares refined using PIRUM (7): $a = 6.341(1)$ Å, $b = 16.880(2)$ Å,

TABLE 4
Atomic Coordinates and Thermal Parameters with Their Standard Deviations for the Neutron Model

Atom	x	y	z	B_{iso} (Å ²)
Sr	0.8786(5)	0.4184(2)	0.7385(6)	0.61(5)
C1	0.6300(6)	0.2384(2)	0.5764(6)	0.71(6)
C2	0.5849(5)	0.5177(2)	0.0912(6)	0.49(5)
C3	0.6495(6)	0.2790(2)	0.3378(6)	0.69(6)
O1	0.6171(7)	0.2290(3)	0.1597(9)	1.35(8)
O2	0.6749(8)	0.2813(3)	0.7532(8)	1.34(8)
Ow3 ^a	0.8613(7)	0.5630(3)	0.5715(8)	1.12(8)
O4	0.7759(6)	0.5072(2)	0.0679(8)	1.14(8)
O5	0.5734(7)	0.1682(3)	0.5661(8)	1.19(8)
O6	0.5139(7)	0.5549(2)	0.2612(9)	1.45(9)
O7	0.6978(8)	0.3493(3)	0.3315(9)	1.58(8)
Dw1 ^a	0.7804(8)	0.0700(3)	0.0219(9)	2.61(9)
Dw2 ^a	0.6317(9)	0.1041(3)	0.8019(9)	2.59(9)
D3	0.1473(9)	0.2456(3)	0.5027(9)	3.0(1)

^a Index w is used to indicate the atoms composing the water molecule.

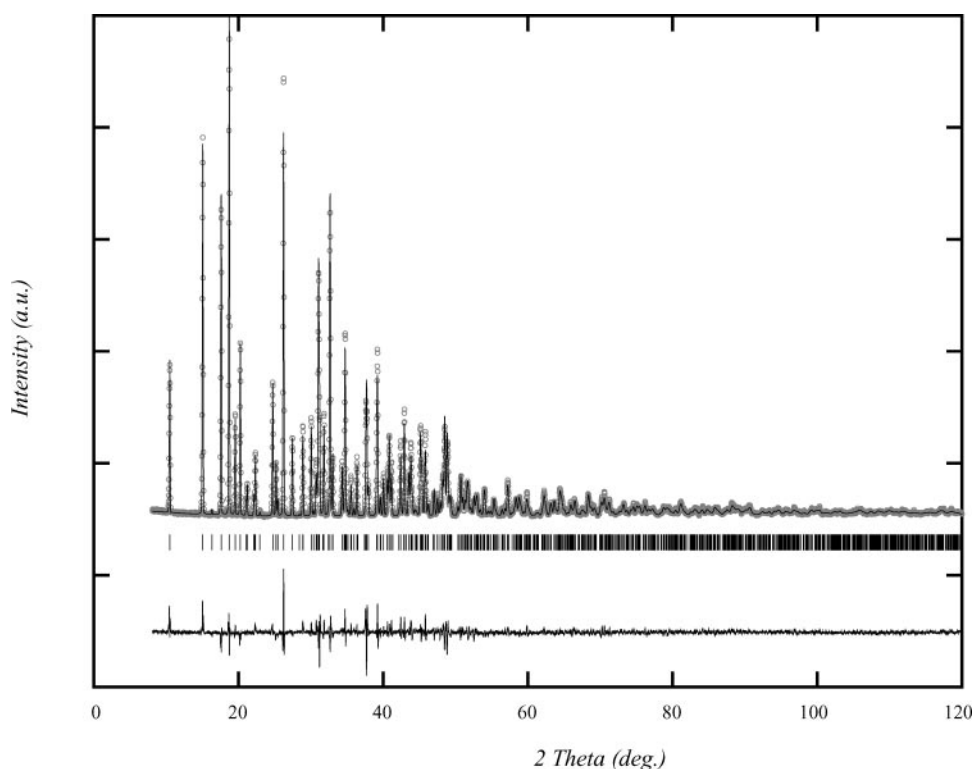


FIG. 1. Rietveld refinement of X-ray data, final difference plot (13).

$c = 5.7798(8) \text{ \AA}$, and $\beta = 97.60(1)^\circ$. The space group $P2_1/n$ was found by studying the systematic absences with the program FULLPROF (8) in profile matching mode (9). From the experimental density and cell volume the number of molecules per unit cell was calculated to be 3.95, which is close to 4. This means 44 nonhydrogen atoms per unit cell altogether. All the above-mentioned results were used as input for the direct methods program EXPO (10), which is the integration of EXTRA (for structure factor amplitude extraction) and SIRPOW92 (for structure determination). In the first model obtained, one carbon atom had to be relabeled as oxygen. This fragment information was recycled again and yielded all nonhydrogen atoms, with $R_{\min} = 6.44\%$. This model, together with the profile parameters obtained from the full pattern matching, was used as a starting point for Rietveld refinement with FULLPROF. Positions and isotropic thermal parameters (54 parameters in total) were refined, constraining B_{iso} for identical atomic species to be the same. Results of the refinement are summarized in Tables 2 and 3, and the final difference plot is shown in Fig. 1.

Neutron Powder Diffraction (NPD)

Neutron powder diffraction experiments were performed for two reasons: first, to check the reliability of the XPD

model and second, to complete the model by including the H/D atoms in order to find in which way the excess of oxalic acid is incorporated in the structure. A run of the data through the direct methods package EXPO did not yield a clear view of the atomic positions, as was the case with the X-ray data. Therefore, neutron data were only used for refinement purposes. The X-ray model was selected as the initial model from which to start. Obviously, without the D atoms incorporated, the initial difference plots looked rather bad ($R_B \sim 18\%$). Difference Fourier maps were then calculated with the program GFOURIER (11). Three clear peaks, at $1.044(8) \text{ \AA}$ from Ow (height $0.078 (10^{-12} \text{ cm})/\text{\AA}^3$), at $1.012(6) \text{ \AA}$ from Ow (height $0.056 (10^{-12} \text{ cm})/\text{\AA}^3$), and at $1.05(1) \text{ \AA}$ from O1 (height $0.061 (10^{-12} \text{ cm})/\text{\AA}^3$), were observed. Because of their positions, they were included in the refinement as deuterium atoms. In the first cycles this was done using constrained positional and thermal parameters for D; afterward these parameters were refined freely. The R_B factor dropped immediately by several percent and refinement converged to the final values, summarized in Tables 2 and 4. The difference plot is shown in Fig. 2. The final Fourier difference map was quite smooth, with min/max between -0.012 and $0.016 (10^{-12} \text{ cm})/\text{\AA}^3$ (at $0.067(4) \text{ \AA}$ from O4).

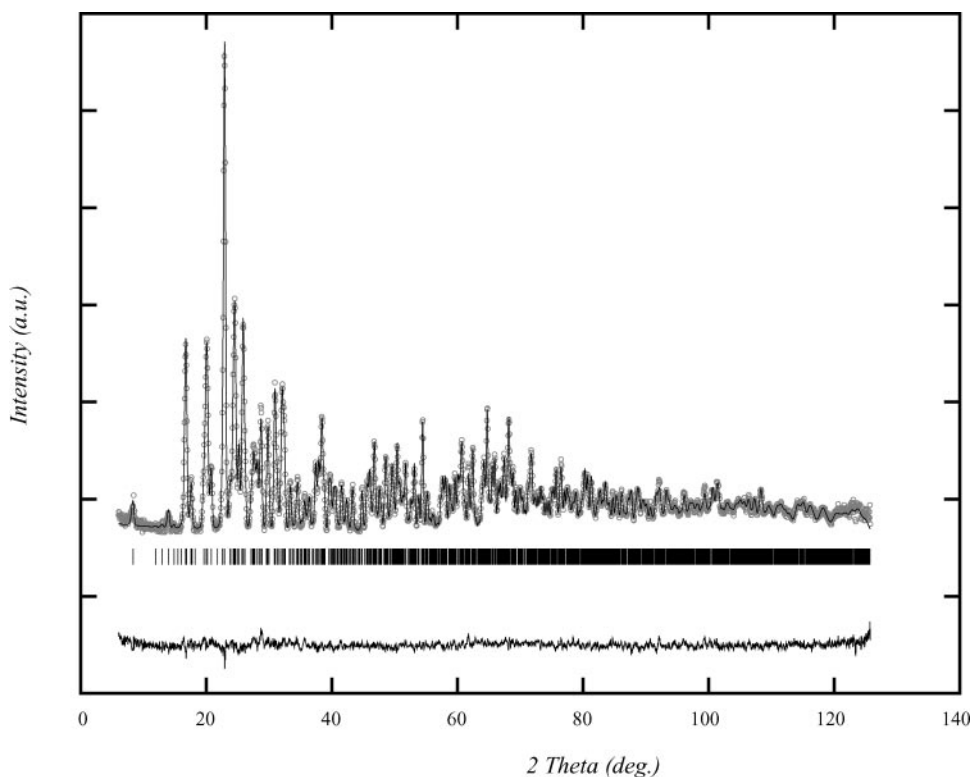


FIG. 2. Rietveld refinement of neutron data, final difference plot (13).

DISCUSSION

Comparison of positional and thermal parameters makes it clear that especially x , z , and B_{iso} of the light elements are more accurately defined with neutrons (lower esd's).

In contrast to what was expected in advance, it is not found that oxalic acid is simply incorporated into the structure compared to $\text{SrC}_2\text{O}_4 \cdot \text{H}_2\text{O}$. In fact, oxalate and hydrogen oxalate anions are present in such a way that each asymmetric unit contains exactly one molecule with structural formula $\text{Sr}(\text{HC}_2\text{O}_4) \cdot \frac{1}{2}(\text{C}_2\text{O}_4) \cdot \text{H}_2\text{O}$ instead of $\text{Sr}(\text{C}_2\text{O}_4) \cdot \frac{1}{2}(\text{H}_2\text{C}_2\text{O}_4) \cdot \text{H}_2\text{O}$ (4).

Completely in accordance with the other known strontium oxalates, Sr is eight-fold coordinated by O. In this coordination sphere (Fig. 3), both the oxalate and hydrogen oxalate anions act once as bidentate and once as monodentate. The two remaining positions are occupied by H_2O molecules. The SrO_8 polyhedron can be described as a distorted bicapped trigonal prism, with $\text{O7} \cdots \text{O2} \cdots \text{O5} \cdots \text{Ow3}$ forming the square face. These polyhedrons are connected to each other only by edge sharing to form one-dimensional chains along the c -axis. The common edges are $\text{O4} \cdots \text{O4}'$ and $\text{Ow3} \cdots \text{Ow3}'$ (Fig. 4), which means that H_2O acts as a bridging ligand between two Sr atoms. This is in contrast to all other Sr oxalates, where H_2O is also coordinated to Sr, but without any bridging function. In the

ac plane, the polyhedra chains are connected by the $\text{C}_2\text{O}_4^{2-}$ groups, while in the bc plane the connection is made by the HC_2O_4^- groups. In addition, there is the possibility to form intrachain ($\text{Dw2} \cdots \text{O5}$ and $\text{D3} \cdots \text{O2}$ along the bc plane) as

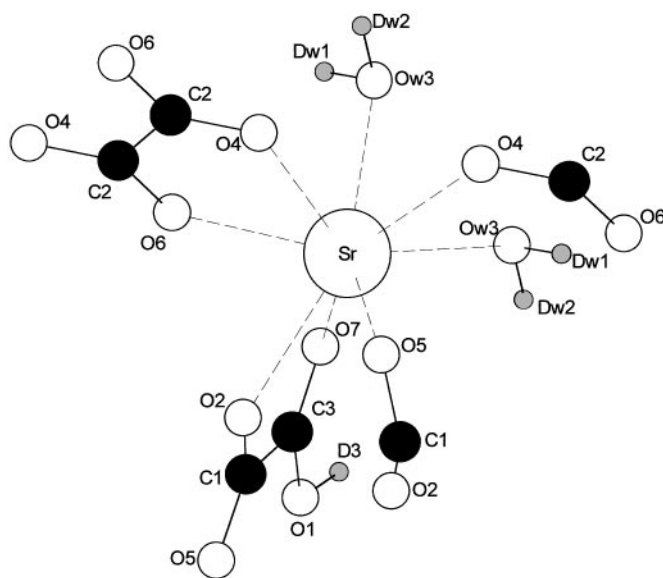


FIG. 3. SrO_8 polyhedron (14).

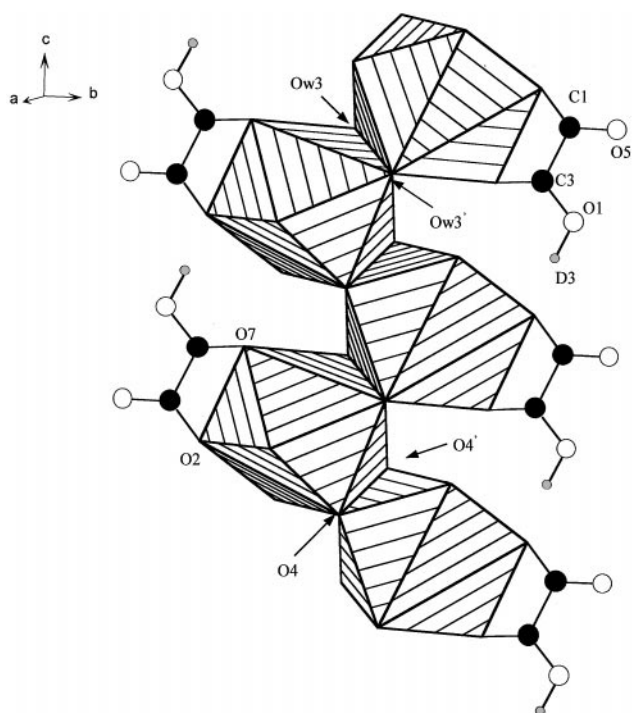


FIG. 4. Connectivity of the SrO_8 polyhedra by edge sharing (14).

TABLE 5
Interatomic Distances (\AA) and angles ($^\circ$) Calculated
According to the Neutron Model

Sr-O2	2.657(6)	O5-C1-C3	115.7(4)
Sr-Ow3 ^a	2.61(1)	O2-C1-C3	115.5(3)
Sr-Ow3' ^a	2.622(6)	O7-C3-C1	120.0(4)
Sr-O4	2.574(7)	O1-C3-C1	112.6(3)
Sr-O4'	2.64(1)		
Sr-O5	2.58(1)	O4-C2-C2'	118.4(3)
Sr-O6	2.530(6)	O6-C2-C2'	115.4(3)
Sr-O7	2.74(1)		
		O1-D3	1.044(8)
C1-O5	1.237(6)	Ow3-Dw1 ^a	0.992(8)
C1-O2	1.254(6)	Ow3-Dw2 ^a	1.005(7)
C1-C3	1.560(5)		
C3-O1	1.326(6)	Dw1-Ow3-Dw2 ^a	105.3(6)
C3-O7	1.227(6)		
		D3...O2	1.544(7)
C2-O4	1.249(5)	Dw1...O6 ^a	1.71(1)
C2-O6	1.296(7)	Dw2...O5 ^a	1.741(8)
C2-C2'	1.526(9)		

^a Index w is used to indicate the atoms composing the water molecule.

well as *interchain* ($\text{Dw1} \cdots \text{O6}$ along the *ac* plane) hydrogen bridges, which give the whole network an extra stability. Interatomic distances and angles are summarized in Table 5.

Up to now, in the anhydrous and hydrated Sr oxalates, three types of oxalate coordination modes were found. Adopting the nomenclature of Price *et al.* (2), in this acid

strontium oxalate a type 2 coordination mode exists. However, a new mode (called type 4), which deals with the HC_2O_4^- group, is found here in equal proportions (Fig. 5). Interesting to notice is the fact that the HC_2O_4^- group, like the $\text{C}_2\text{O}_4^{2-}$ group, is almost planar. From a theoretical study (12), it was expected that in salts with rather bulky cations, the orthogonal conformer might be the preferred form, although the calculated energy difference between the two conformers was quite low ($\sim 1.6 \text{ kcal mol}^{-1}$).

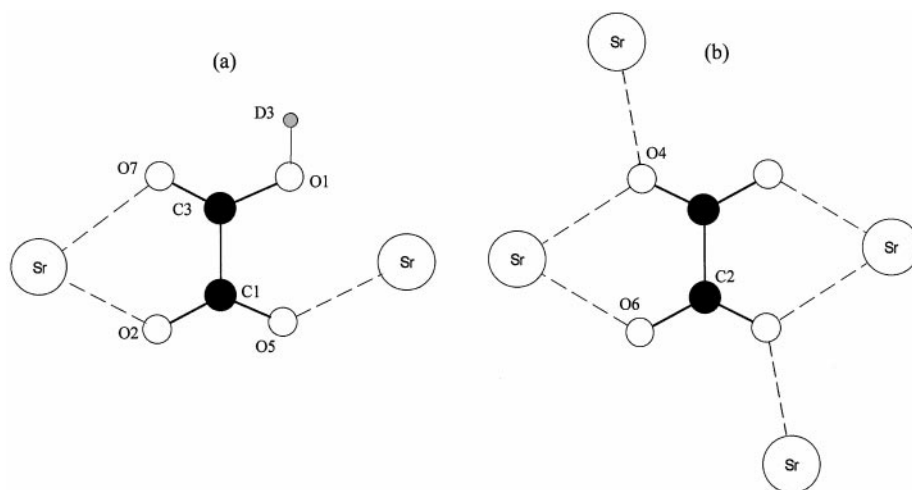


FIG. 5. Coordination types in acid strontium oxalate: (a) type 4 and (b) type 2 (14).

ACKNOWLEDGMENTS

G.V. and M.K.V.B. are respectively Research Assistant and Post-doctoral Fellow of the Fund for Scientific Research–Flanders (Belgium) (F.W.O.). Prof. Dr. S. Hoste (Vakgroep Anorganische en Fysische Chemie, RUG, Belgium) is acknowledged for providing the experimental density data. The experiment at the LLB was supported by the European Commission through the TMR-LSF (Training and Mobility of Researchers–Access to Large Scale Facility) Program (Contract No. ERB FMGE CT 95 0043).

REFERENCES

1. “Structure Determination from Powder Diffraction—Database,” A. Le Bail, available at URL <http://www.cristal.org/iniref.html>.
2. D. J. Price, A. K. Powell, and P. T. Wood, *Polyhedron* **18**, 2499–2503 (1999).
3. A. N. Christensen and R. G. Hazell, *Acta Chem. Scand.* **52**, 508–512 (1998).
4. E. Knaepen, J. Mullens, J. Yperman, and L. C. Van Poucke, *Thermochim. Acta* **284**, 213–227 (1996).
5. P. E. Werner, L. Eriksson, and M. Westdahl, *J. Appl. Crystallogr.* **18**, 367–370 (1985). Treor97 is an evolution of the well-known Treor90 indexing program.
6. A. Boulif and D. Louër, *J. Appl. Crystallogr.* **24**, 987–993 (1991).
7. P. E. Werner, *Ark. Kemi* **31**, 513–516 (1969) (Version 921204).
8. J. Rodriguez-Carvajal, “Abstracts of the Satellite Meeting on Powder Diffraction of the XVth Congress of the International Union of Crystallography, 127 (Toulouse, 1990),” Version 3.5d.
9. A. Le Bail, H. Duroy, and J.-L. Fourquet, *Mater. Res. Bull.* **23**, 447–452 (1988).
10. A. Altomare, M. C. Burla, G. Cascarano, C. Giacovazzo, A. Guagliardi, A. G. G. Moliterni, and G. Polidori, *J. Appl. Crystallogr.* **28**, 842–846 (1995).
11. J. Gonzales-Platas and J. Rodriguez-Carvajal, “GFOURIER a windows program for Fourier maps in crystallography,” available at URL <http://www-llb.cea.fr/fullweb/others/newfour.html>.
12. M. J. S. Dewar and Y. J. Zheng, *Theochem.* **209**, 157–162 (1990).
13. T. Roisnel and J. Rodriguez-Carvajal, “WinPLOTR a new tool for powder diffraction,” available at URL <http://www-llb.cea.fr/winplotr/winplotr.html>.
14. K. Brandenburg (Crystal Impact GbR.), “DIAMOND: Visual Crystal Structure Information System,” version 2.1c.